SEVERAL TSUNAMI SCENARIOS AT THE NORTH SEA AND THEIR CONSEQUENCES AT THE GERMAN BIGHT

Silvia Chacón-Barrantes
Departamento de Física, Universidad Nacional de Costa Rica, Heredia, COSTA RICA
Now at the Coastal Research Laboratory, University of Kiel, GERMANY
email: silviachaconb@gmail.com

Rangaswami Narayanan
Formerly, Reader, Department of Civil and Structural Engineering, University of Manchester, Manchester, UNITED KINGDOM.

Roberto Mayerle
Coastal Research Laboratory, University of Kiel, GERMANY

ABSTRACT

Tsunamis occurred in the past at the North Sea, but not frequently. There are historical and geological records of several tsunamis: the Storegga tsunami caused sediment deposits in Scotland 8,000 years ago and records of at least six earthquake-generated tsunamis exist from 842 to 1761 AC. The highest tsunami height witnessed at the German Bight is comparable to the maximum storm surge recorded and could thus cause similar or higher damage. However, there is little research on tsunami modeling in the North Sea. Here, we performed ten numerical experiments imposing N-waves at the open boundaries of a North Sea model system to study the potential consequences of tsunamis for the German Bight. One of the experiments simulated the second Storegga slide tsunami, seven more explored the influence of the incidence direction of the tsunami when entering the North Sea domain, and the other two explored the influence of tides on tsunami heights. We found that the German Bight is not exempt from tsunami risk. The main impact was from waves entering the North Sea from the north, even for tsunamis with sources south of the North Sea. Waves entering from the English

Vol. 32, No. 1, page 8 (2013)

Channel were attenuated after crossing the Dover strait. For some scenarios, the tsunami energy got focused directly at the Frisian Islands. The tidal phase had a strong influence on tsunami heights, although in this study the highest heights were obtained in the absence of tides. The duration of tsunamis is significantly smaller than that of storm surges, even though their flow velocities were found to be comparable or larger, thus increasing their possible damage. Therefore, tsunamis should not be dismissed as a threat at the North Sea basin and particularly at the German Bight.

1. INTRODUCTION

Tsunamis are not frequent in the North Sea; nevertheless, there is plenty of evidence of impact of tsunamis originating both inside and outside the North Sea basin. Many of the tsunamis had only local impact and were generated by slides in fjords, whereas others were of far reaching impact, caused by submarine slides and earthquakes. The most renowned tsunami in the North Sea was generated by the second Storegga submarine slide about 8,000 years ago in the Norwegian Sea (Harbitz, 1992). Besides this event, the NOAA Global Historical Tsunami Database (NGDC/WDC, 2012) includes tsunamis in Germany and Denmark in 1760 and in the United Kingdom and France in 842 and 1580 which were attributed to local earthquakes. Also, there are reports in this database for tsunamis in the United Kingdom, France and the Netherlands in 1755 and 1761 caused by earthquakes from the offshore area of Portugal in the Atlantic (NGDC/WDC, 2012).

To the authors' knowledge, two modeling studies on tsunamis in the North Sea have been performed to date – one by Borck et al. (2007) and the other one by Lehfeldt et al. (2007). Both studies obtained tsunami heights of less than 2m and therefore concluded that the tsunami risk is not high for the German Bight because of the shallow depths of the North Sea and because of the protection provided by Norway and the British Islands. Nevertheless, Newig and Kelletat (2011) put together several reports along the North Sea basin to demonstrate that there was a tsunami on 5 June 1858, which caused run-ups of up to 4m in Germany, specifically in Sylt, Helgoland and Wangerooge. Tsunami heights between 1.2 and 6m were reported also in the United Kingdom, France, the Netherlands and Denmark. There were no casualties reported because the summer season had not yet started and tourism was scarce at that time. Still, several people, mostly in fishing communities, were reported to have barely escaped the onslaught of the tsunami (Newig and Kelletat, 2011).

For their tsunami model, Borck et al. (2007) used as input "three successive positive single waves" generated by a sine-square function. The use of three solitary waves together has no physical meaning, as they are not a good representation of the leading tsunami wave. Lehfeldt et al. (2007) used a square hyperbolic secant solitary wave as input and imposed it perpendicularly at the open boundaries. Even when solitary waves are accepted as a representation of the leading tsunami wave, better results were obtained using N-waves to represent tsunamis because of their bipolarity

(Tadepalli and Synolakis, 1996). The reports of the 1858 tsunami in the English Channel draw attention to a withdrawal of the sea followed by inundation (Newig and Kelletat, 2011). Therefore, for this work, N-waves are used to represent the leading wave of tsunamis.

Our work described in this paper involved ten experiments in order to explore the tsunami risk in terms of run-up for the German Bight under a wider and more realistic approach. As it is well known, earthquakes are the most common source of tsunamis in the world and earthquake-generated tsunamis differ from those generated by landslides - both in amplitude and frequency. Consequently, we considered one case of a landslide-generated tsunami with normal incidence and seven cases of earthquake-generated tsunamis with various directions of incidence. In all these cases, tides were not considered in the modeling. To explore the role of tides on tsunami heights, we performed two more experiments which included tides in the calculations.

2. THE MODEL SYSTEM

For this work, we utilized a model system based in Delft3D software, which is a finite differences numerical model able to simulate coupled flow, sediment transport and morphodynamic processes. The model solves the non-linear shallow water equations using an alternating implicit scheme (Leeser et al., 2004). This package has been validated and verified for tsunami propagation and run-up (Apotsos et al., 2011a) and it has been employed in several one-dimensional tsunami studies like Apotsos et al. (2011b), (2011c), Apotsos et al. (2009) and Gelfenbaum et al. (2007), and two-dimensional tsunami studies like Vatvani et al. (2005).

Specifically for this study, we modified an existing model system which covers the entire North Sea. The model system consists of four, two-dimensional, nested models: a) the Continental Shelf Model (CSM) from Verboom et al. (1992); b) the North Sea Model (NSM) from Bruss et al. (2010); c) the German Bight (GBM); and d) the Dirthmarschen Bight (DBM) models from Hartsuiker (1997). For the present study, we employed only two models of the system, the NSM and the GBM. The first model covers only the North Sea and it is not capable of computing inundation on dry land. In this model the input waves can be imposed in both the western and the northern open boundaries. The second model, the GBM, covers the German coasts and it is capable of simulating inundation on dry land. The nesting boundaries between the NSM and the GBM are drawn with thick black lines in Figure 1. The resolution of the original NSM varies between 7079.62m and 9349.68m, and the corresponding Imamura numbers vary between 4.64 and 6.25. The Imamura number is defined as:

$$Im = \frac{dx}{2h}\sqrt{1 - gh\left(\frac{dt}{dx}\right)^2} \qquad\qquad 1$$

with dx the grid resolution, dt the time step and h the water depth. The Imamura number relates numerical and physical dispersion on the modeling of tsunami propagation and it should be kept close to one (Imamura and Goto, 1988). As the Imamura numbers of the NSM are much larger than one, we refined this grid by a factor of three. The refined NSM (refNSM) has a resolution between 2359.87m

and 3116.58m. The corresponding Imamura numbers are between 0.72 and 1.57, more appropriate for tsunami propagation.

In the present work the tsunami-like waves were imposed using the Riemann-invariant boundary condition to minimize false reflections in the open boundary (Verboom and Slob, 1984). As the Riemann invariant is calculated with the water level and the flow velocity, for N-waves we used the flow velocity of the shallow water wave theory, U=ηgh, where η is the water level, g is the gravity acceleration and h is the water depth. If an open boundary had no incoming wave then a zero Riemann invariant was prescribed to allow the wave leaving the domain.
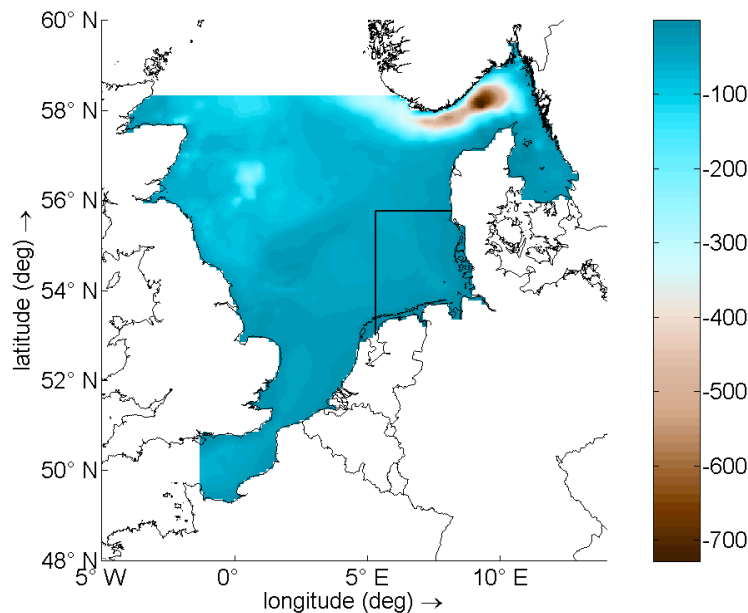

Figure 1. Extent and bathymetry of the model system. The thick black lines show the boundaries between the German Bight Model (GBM) and the North Sea Model (NSM). The color scale is in meters of depth.

3. VALIDATION OF REFINED MODEL

The nesting between CSM and GBM was validated by Mayerle et al. (2005), later by Bruss et al. (2010) which splitted the CSM and defined the NSM. As the NSM consists on a section of the CSM and has the same resolution, the nesting between the NSM and the GBM is the same as between the CSM and the GBM. Nevertheless, as we refined the North Sea grid for tsunami propagation purposes, the nesting between the refNSM and the GBM needed to be validated. For this purpose, we performed simulations of three large storms at the North Sea, which occurred in 1967, 1976 and 1999 with the original and refined North Sea models. Additionally, the mild weather conditions from April 2008 were simulated to include more general scenarios. To test the nesting of the refNSM with the GBM we compared its results with results from the NSM nested to the GBM, as this original nesting has been extensively validated with field data (Mayerle et al., 2005; Bruss et al., 2010).

For all validation cases, air pressure and wind fields were imposed in both North Sea models and the results were used as input, together with air pressure and wind fields, for the GBM. The percentage difference between the maximum water heights calculated by both models at the German Bight was smaller than 3% for the whole domain in all cases, indicating that the differences between results from both model systems are negligible, and that the refNSM can be nested to the GBM using the same procedure as for the original model system.

4. STOREGGA-LIKE TSUNAMI

In the first tsunami experiment, we modeled the second Storegga tsunami. Harbitz (1992) modeled the tsunamis caused by the first and second Storegga slides in the Norwegian Sea 8000 years ago. His resultant time series of water level for the second slide in offshore Aberdeen, Scotland (his station 8), shows a leading depression N-wave with maximum amplitudes of about 2.5m. The time between the maximum depression and maximum elevation is about 96min. To reproduce such a wave we used the formulation of landslide N-waves by Carrier et al. (2003):

$$\eta(t) = a_1 e^{-k1\cdot(t-t1)^2} - a_2 e^{-k2\cdot(t-t2)^2} \qquad 2$$

where η is the water level perturbation, t is the time, and for the constants the following values were assigned: a1=2.35m, a2=2.61m, k1=0.00125min-1, k2=0.001min-1, t1=471min and t2=381min. The resulting wave is plotted with a solid line in Figure 2. This wave matches Harbitz (1992) modeling, drawn as a dashed line in the same figure. This N-wave defined the boundary condition for a tsunami generated by a landslide, imposed normal to the northern boundary of the refNSM. No wave was imposed at the western boundary.
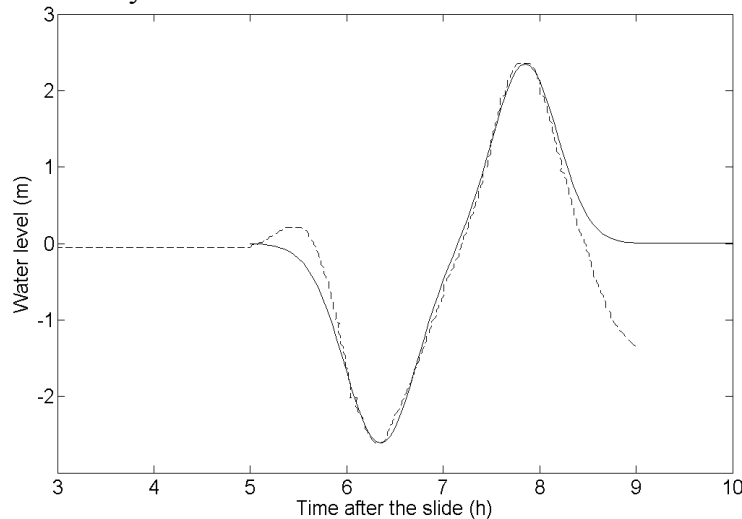

Figure 2. Water level of the N-wave imposed as boundary condition (solid line) for the Storegga-like experiment. The results from Harbitz (1992) for the second Storegga slide are shown with a dashed line.

The bathymetry used in the model during the simulations was the present bathymetry. The mean sea level nowadays is not the same as 8000 years ago, and neither is the bathymetry. Therefore, the goal of this experiment was not to obtain accurate calculations of the historical tsunami run-up but only the consequences for the German Bight if the same tsunami would happen today. As the North Sea Model is not capable in calculating the inundation of dry land, the maximum tsunami heights were computed for the offshore area. However, because of the shoaling effect, the corresponding run-ups should be expected to be larger.

Maximum water levels of more than 5m over the mean sea level were obtained at Inverness and Edinburgh (Firth of Forth), Scotland. These results match those of Smith et al. (2004) who concluded that the run-up of the second Storegga tsunami in inlets at Scotland mainland, probably exceeded 5m over the local mean high water mark of spring tides at that time, while it was probably less along the open coast. Figure 3, left side, illustrates the computed maximum tsunami heights along the entire North Sea basin, roughly confirming these estimates.
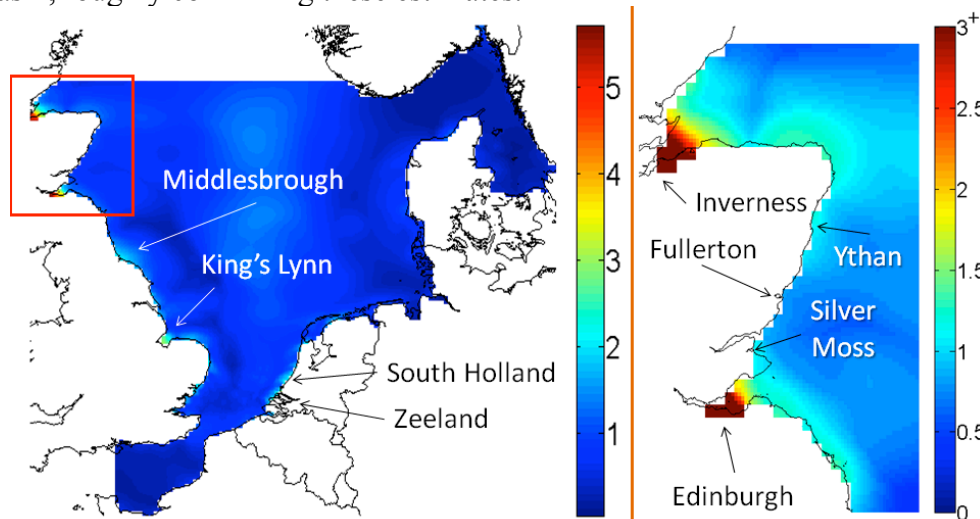

Figure 3. Left side: Maximum tsunami heights in meters at the whole North Sea basin for the Storegga-like tsunami, the red rectangle shows the detailed area at the right side where deposits from Storegga tsunami have been identified. At the right side the color scale is saturated to depict more details.

At the right hand side of Figure 3 the maximum tsunami heights are shown along the British coasts where tsunami deposits from Storegga event have been identified. At the open coast site of Waterside (mouth of the river Ythan), maximum offshore heights of 1-1.5m were obtained. Here the maximum height of the sediment deposits is also about 1-1.5m (Smith et al., 2004). According to Dawson (1999), the height of sediment deposits is lower than the maximum tsunami run-up and considering that run-up should be larger than offshore tsunami heights, our calculations are satisfactory in this point. In small inlets the model results underestimated the tsunami heights. The tsunami deposits suggest a minimum run-up of about 4m in Fullerton (Smith et al., 2004) and our model reproduces about 1m of maximum offshore tsunami height. At Silver Moss, the tsunami deposits point to a

minimum tsunami run-up of about 2m (Smith et al., 2004) and our model calculated about 1.3m of maximum offshore tsunami height. Together with the lack of correct bathymetry, there is another reason for these differences. Specifically, the refNSM does not include these inlets completely because of its resolution. Also, the refNSM does not consider inundation of dry land; therefore the interaction of the tsunami with the coast is not well solved. At small inlets this interaction determines greatly the tsunami heights. Smith et al. (2004) postulated that the Storegga tsunami also impacted the U.K. shorelines south of where the tsunami deposits were found. Our model system predicted offshore tsunami heights above 2m in places like Middlesbrough and King's Lynn (Figure 3 left side). Maximum offshore tsunami heights of over 2m were also obtained in the south coast of the Netherlands, offshore South Holland and Zeeland - although no sediment deposits have been found in these places.

Figure 4 illustrates the simulated maximum tsunami heights in the whole German Bight domain for a Storegga-like tsunami. The highest values of almost 2m were obtained for the Western Frisian Islands, specifically at Schiermonnikoog and Ameland, and smaller values of about 1m were obtained for the Northern Frisian Islands, particularly for Sylt. Figure 5 shows water level time series for the six German stations in the regions of higher tsunami heights. Among these stations, the highest water level of almost 1.0m was computed in Westerland, Sylt Island. Despite the fact that the tsunami heights seemed to be not high enough to pose a risk to German coasts, all the time series depicted in Figure 5 have a leading depression shape, which usually implies larger onshore velocities (Pritchard and Dickinson, 2008), which can cause greater damage.
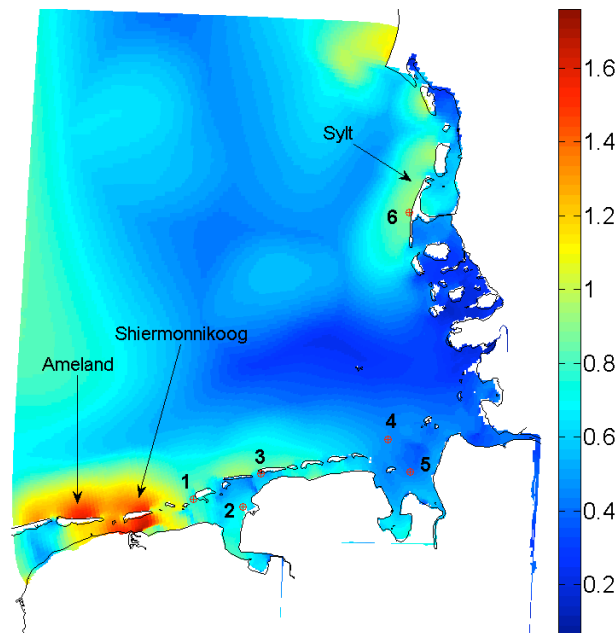

Figure 4. Simulated maximum tsunami heights in meters in the German Bight Model for the Storegga-like tsunami. The red crossed circles show the localization of the German stations where the highest tsunami heights were obtained: 1. Borkum, 2. Leybuch, 3. Norderney, 4. Alte Weser, 5. Dwarsgat and 6. Westerland.
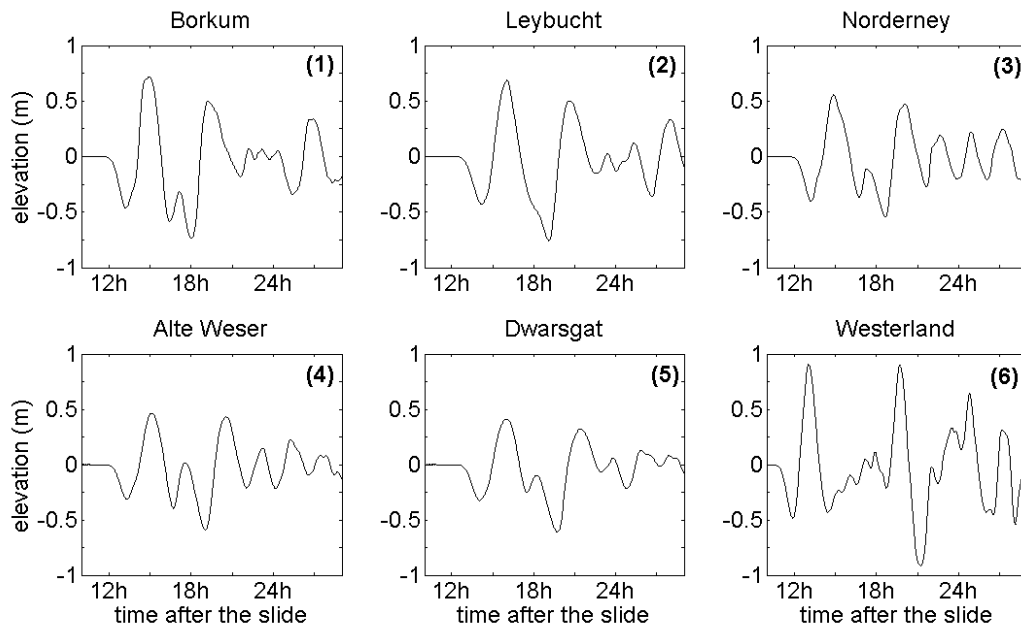
Figure 5. Simulated time series of tsunami heights at six stations on the German coast for the Storegga-like tsunami. The localization of the stations is shown in Figure 4. The time is given in hours after the event and in all plots water elevation is given in meters over the mean sea level.

5. EARTHQUAKE-GENERATED TSUNAMIS

The risk of earthquake-generated tsunamis was evaluated in separate experiments, using different forcing functions from a landslide-generated tsunami. First, we considered the case of the wave entering only from the western boundary. Additionally, we considered six different directions of incidence for the wave at the northern boundary, to explore the effect of incidence directions on the focusing of the tsunami energy and the many possible sources for earthquake-generated tsunamis. Two of the incidence directions that were used corresponded to the historical 1755 Lisbon and the 1929 Grand Banks tsunamis. Earthquakes generated both of these tsunamis, however in the case of Grand Banks, the earthquake was followed by a submarine landslide.

For all the cases considered in this section, we used symmetric leading depression N-waves as input, similar to the Tadepalli and Synolakis (1996) formulation:

$$\eta(t) = \frac{3\sqrt{3}}{2} H \cdot \mathrm{sech}^2[\gamma(t - t_0)] \cdot \tanh[\gamma(t - t_0)] \qquad\qquad 3$$

In Eq. 3 η is the water level perturbation, H is the wave height, t is time, t0 is the midpoint of the wave, $\gamma = \frac{3}{2}\alpha \cdot \sqrt[4]{\frac{3}{4}A}$ and α is a constant which determines the width of the wave. Because of

the date of the tsunamis referred above, no data is available on the height or the width of the incoming waves. Nevertheless, for the 1858 event, the water was reported to recede and then come back in 5-7min, in Bologne-sur-Mer and in Le Havre, in the English Channel. Consequently, we chose t0=20min and γ=0.2087min-1 to have 6min between the depression and the peak of the N-wave. Although N-waves are non-periodic waves, Synolakis et al. (2008) define an equivalent wavelength as the distance between the points where the wave height is 1% of its maximum value at the beginning and at the end of the N-wave. Using this definition, the equivalent period of our wave was 33.2min, typical of the earthquake-generated tsunamis. A unitary height was used for the incoming waves because the goal of this section was to identify the vulnerable regions and the wave height amplification.

6. IMPACT OF THE WESTERN WAVE

In this experiment, the wave was imposed only at the western boundary of the refNSM (Figure 1). Tsunami heights of 1-2m were obtained at Bognor Regis at the English Channel (not shown). By comparing wave heights before and after crossing the Dover Strait, the western wave was highly attenuated after passing through this strait. The wave just before and just after crossing the strait is shown in Figure 6, at points with similar depths of about 36m. The maximum heights after crossing the strait were less than half of those before crossing. With an incoming wave of unitary height at the mouth of the English Channel, the maximum wave height after the Dover strait was about 10cm. This strong damping implies that there should be almost no interference between a wave entering the domain through the west and a wave entering the domain through the north.
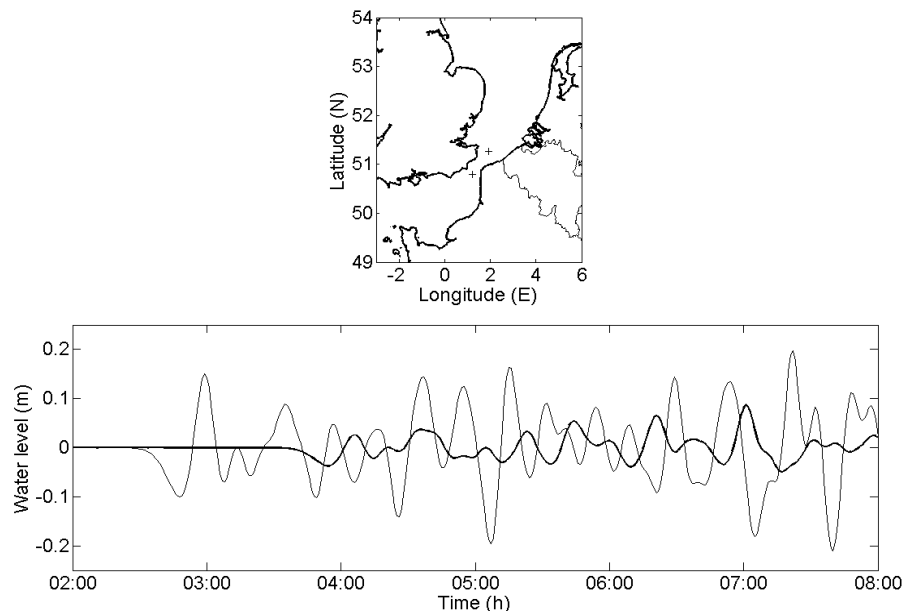

Figure 6. Bottom: Comparison of the western wave just before (thin line) and just after (bold line) crossing the Dover strait. Top: Location of the points where the wave was calculated. Both points have depths of around 36m.

6.1 Influence of the direction of incidence of the northern wave

We considered two scenarios of earthquake-generated tsunamis based on the NOAA travel time maps of the 1755 Lisbon and 1929 Grand Banks events plotted in Figure 7 (NGDC, 2012). Other authors propose different locations for the 1755 Lisbon earthquake, as usually happens for large earthquakes. In this case in particular, there were no seismograms recorded that contribute to locate the event. These two historical tsunami scenarios differed only in the incidence direction of the wave through the northern boundary. This difference can be seen in Figure 7; the Lisbon tsunami originally came from the south and travelled around Ireland before entering the northern North Sea. The Grand Banks tsunami, on the other hand, came straight from the west, crossing the North Atlantic Ocean before entering the North Sea.
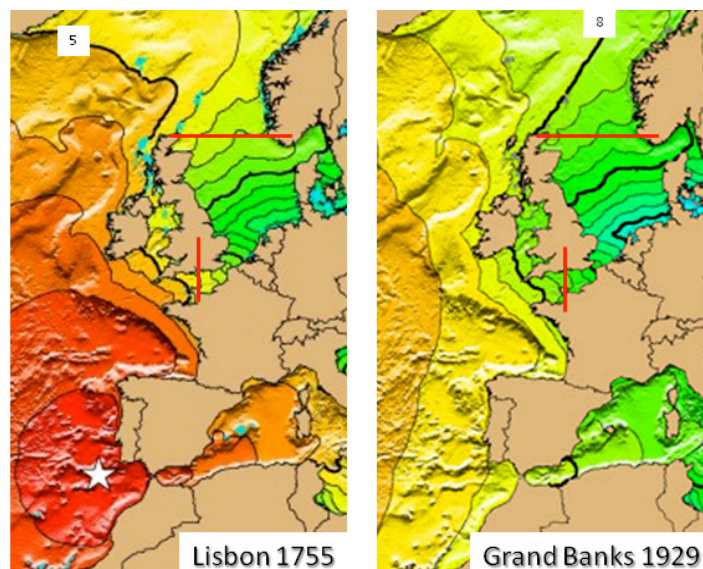

Figure 7. Travel time maps for two historical events arriving to the North Sea taken from the National Geophysical Data Center Tsunami Travel Time Maps website (NGDC, 2012). Time contours are plotted every hour and thick black lines are plotted every five hours (left) and every four hours (right). The numbers represent hours after each earthquake. Red thick lines show the approximate boundaries of the refNSM. The plots contain no information on the tsunami heights, only on its travel times.

As the depth of water along the north open boundary of the refNSM is not uniform, the incidence angle is not the same along this boundary (see time contours at Figure 7) and it is not possible to refer to a wave incidence angle for the various cases. Instead, the direction of incidence of the tsunami was given by means of the difference of arrival times between Wick in Scotland and Rekefjord in Norwegian shores, hereafter referred to as the time of entrance (Te). If a wave enters normally to the open boundary then the elapsed time is zero because it reaches Scotland and Norwegian shores at the same time. Following Figure 7, the time of entrance was Te=183min (=3h3min) for the Lisbon-like scenario, and Te=122min (=2h2min) for the Grand Banks-like scenario. Additionally to these two historical tsunamis, hereafter case (d) and case (c) respectively, we considered four complementary

incidence directions: normal incidence, case (a), and entrance times of 61, 244 and 305min, cases (b), (e) and (f) respectively. For simplicity we decided not to impose waves at the English Channel in this Section, as the results from Section 5.1 showed that a wave entering through the English Channel got highly damped after crossing the Dover strait. Finally, the height of the incoming wave was set to one, in order to present the results in terms of wave amplification rather than in terms of absolute wave height. We found that the incidence direction determined the places where the energy was concentrated. In the North Sea, the higher the time of entrance, the further east the focusing of wave energy (Fig. 8).
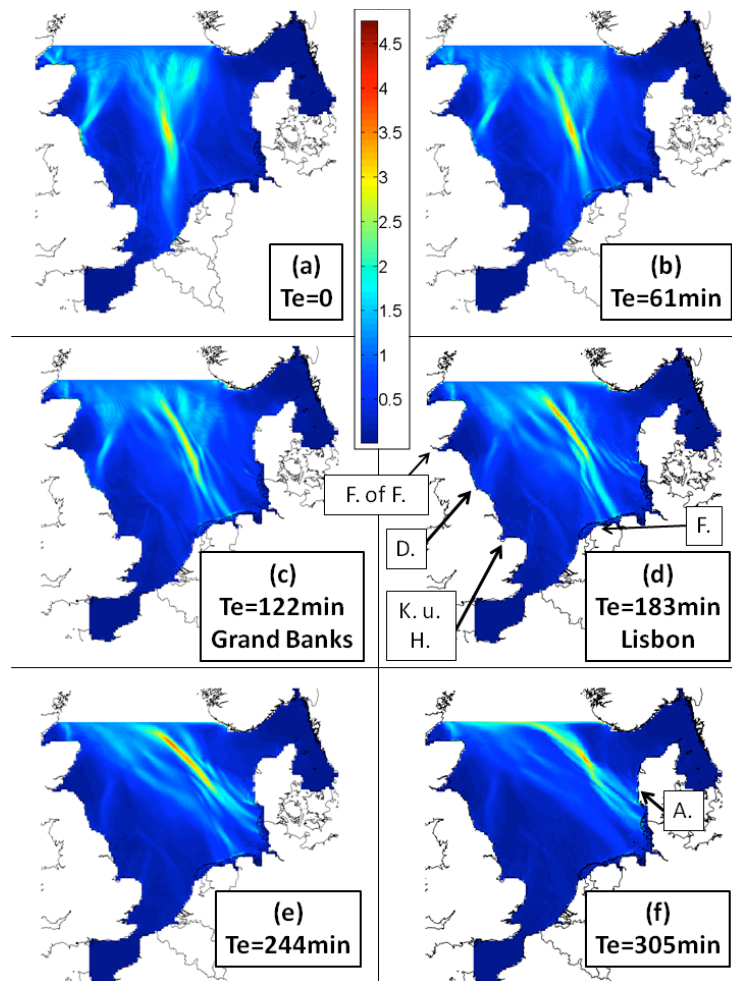

Figure 8. Maximum tsunami amplification factor for different directions of incidence of a unitary N-wave following Tadepalli and Synolakis (1996). Case (a) corresponds to perpendicular incidence. The others have oblique incidence with (b) 61min, (c) 122min (Grand Banks like), (d) 183min (Lisbon like), (e) 244min and (f) 305min time to complete the entrance through the northern boundary. Some geographical places are shown in subfigure (d): Firth of Forth (F. of F.) in Scotland, Durham (D.) and Kingston upon Hull (K. u. H.) in England, and Friesland (F.) in The Netherlands. In subfigure (f) Årgab in Denmark is pointed out.

For all the cases, a certain amount of energy was focused always on the Frisian Islands and North Sunderland in England, although the proportion depended highly on the incidence direction. For all the cases studied in this section, the tsunami heights west of the Dover Straits were negligible.

Important differences were also found due to the forcing type employed. Normal incidence (case a) affected mostly the southern coast of the Netherlands and North Sunderland in England. The Storegga-like tsunami simulated in Section 4 also arrived normal to the north open boundary and affected mostly inlets along Scotland and England.

For the Grand Banks-like tsunami (case c), most of the energy was focused on the East and West Frisian Islands and less on the Durham shores, in England (Figure 8c). For this tsunami, there were no reports of arrival in Germany, Great Britain or France. It is quite possible that the tsunami was significantly damped after crossing the Atlantic Ocean. For the Lisbon-like tsunami (case d), most of the energy was focused on the East Frisian Islands in Germany (Figure 8d). Little energy was focused to the West and North Frisian Islands in the Netherlands, Germany and Denmark and even less to the Durham shores in England. The Global Historical Tsunami Database (NGDC/WDC, 2012) reported the arrival of the Lisbon tsunami at several locations along the east coast of Great Britain, including Firth of Forth in Scotland and Durham and Kingston upon Hull in England. Damaged boats and broken moorings were reported in Friesland, the Netherlands. There are no reports of the tsunami arrival to Germany. Considering the date, the lack of reports might be also due to scarce coastal population or poor record preservation.

At the GBM, the case of completely normal incidence, case (a), presented wave heights of less than one meter, meaning no amplification of the original wave that entered at the North Sea. Case (b) with almost normal incidence, presented the lowest amplification of wave height for the GBM, of less than two. The Lisbon-like scenario (case d) presented the highest amplification among all cases, of more than three times at the north shores of Borkum and Juist Islands. The Borkum station is facing the mud flat behind the island and the water heights computed there were of less than 2m (Figure 10), corresponding to less than twofold amplification. The Westerland station, at the western shore of Sylt Island, registered the highest heights for case (e), which had more tangential incidence than the Lisbon-like case, of almost 2m as shown in Figure 10e.

The seaside of the Frisian Islands presented the highest water levels in all cases (Figure 9), yet the mudflats between the Frisian Islands and the mainland mitigated the impact of the tsunami at continental shores. This mitigation did not happened for the Storegga-like tsunami of Section 4 (Figure 4), another difference due to the waveform. The four cases of more normal incidence (cases a, b, c, and d) presented pronounced focusing of energy to the East Frisian Islands, and the two cases of more tangential incidence (cases e and f) presented more focusing of energy to the North Frisian Islands. The arrival time at each station increased with the incidence direction (Figure 10), the arrival time for the most tangential case (case f) was between 3 and 4 hours higher than for the normal incidence case (case f).

Comparing the results from the two historical tsunamis, the Grand Banks-like tsunami (case c)

presented water heights bellow those for the Lisbon-like tsunami (case d). As we employed incident waves of unitary height in all the cases, it is not only the smaller distance travelled by the tsunami what would make a Lisbon-like tsunami more dangerous than a Grand Banks-like tsunami for the German Bight, but also the orientation of its arrival at the North Sea.
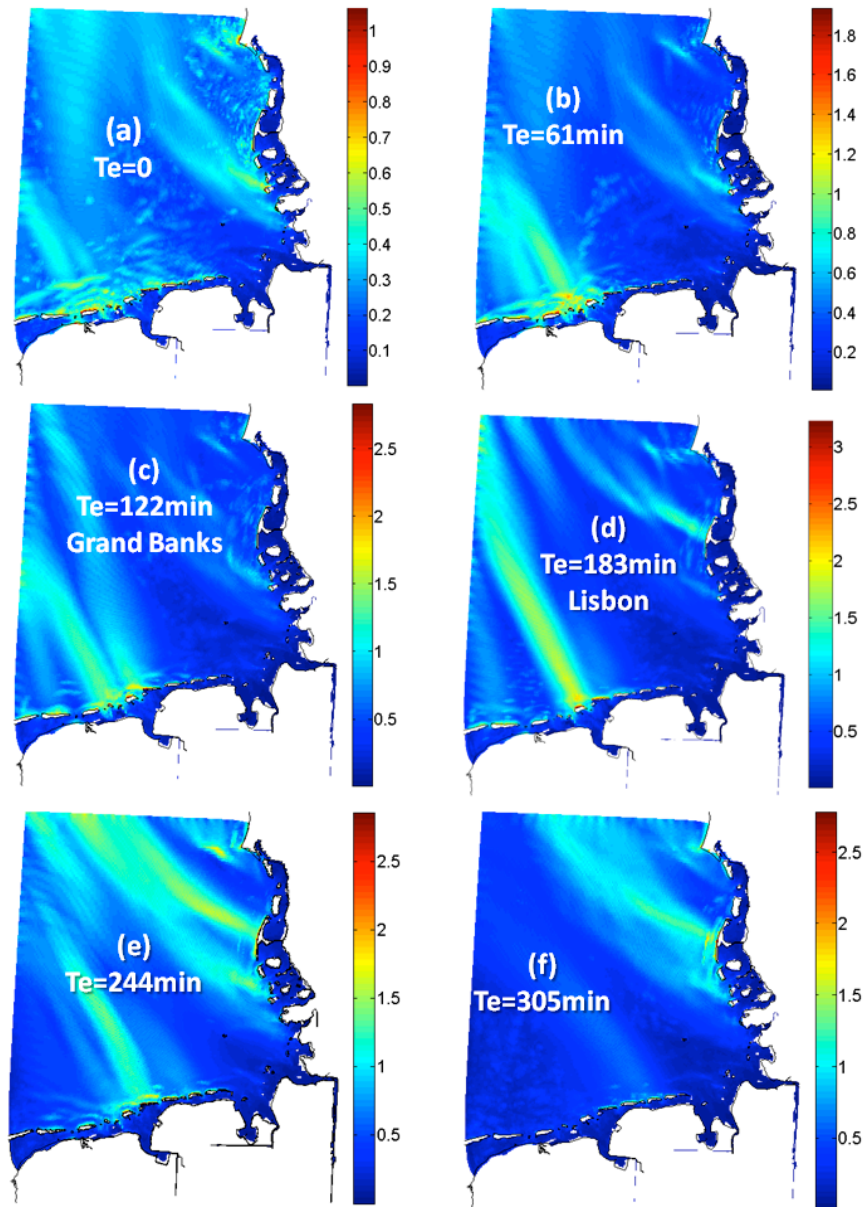

Figure 9. Maximum tsunami heights at the German Bight domain in meters for the various directions of incidence at the refined North Sea Model plotted in Figure 8. Case (a) corresponds to normal incidence. The others have oblique incidence with (b) 61min, (c) 122min (Grand Banks like), (d) 183min (Lisbon like), (e) 244min and (f) 305min time to complete the entrance through the northern boundary of the refined North Sea Model.
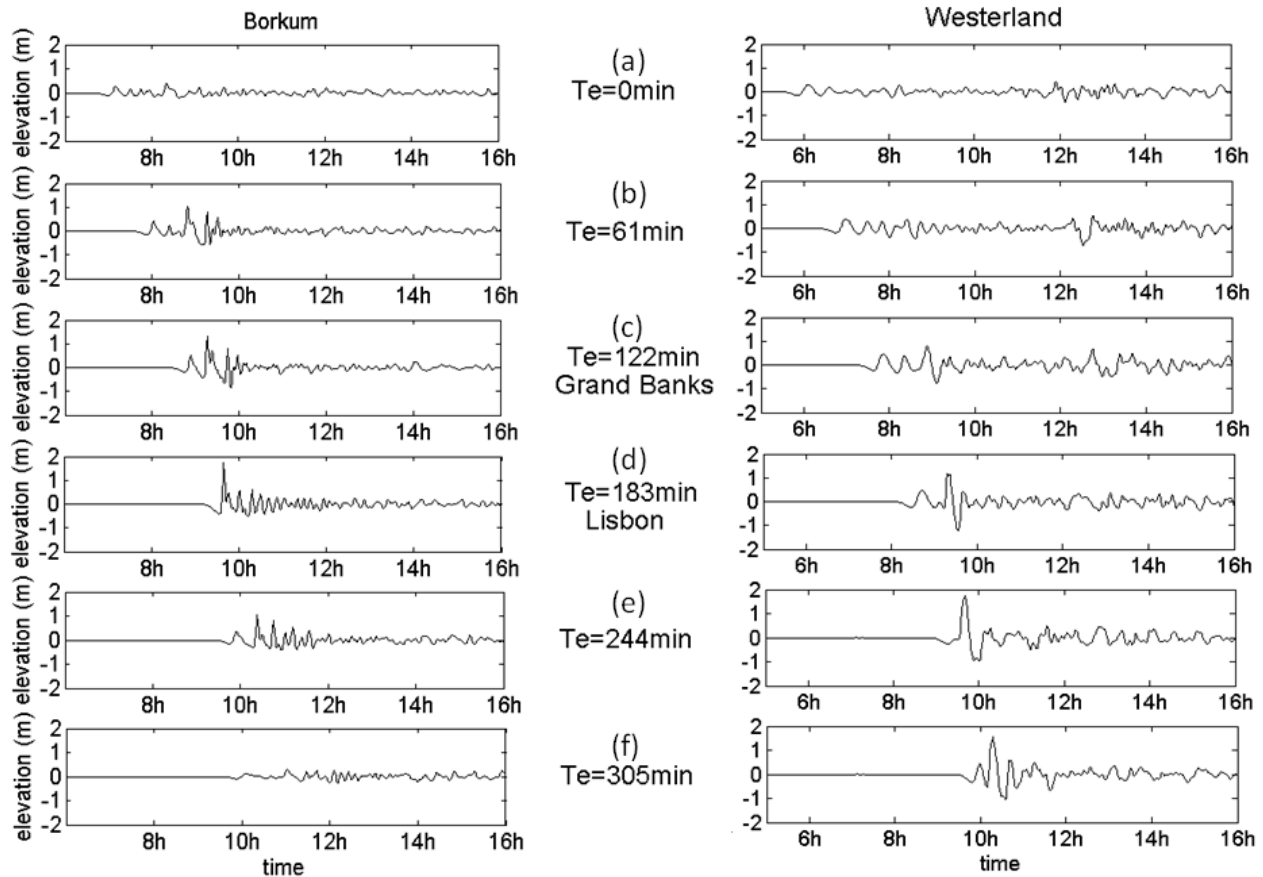
Figure 10. Time series of water height in meters for two stations at the Eastern (left) and Northern (right) Frisian Islands for the six incidence directions through the northern boundary of the refNSM.

7. THE 1858 NORTH SEA TSUNAMI

In 1858 a tsunami arrived to the North Sea from an unknown source. The highest water heights were reported at Wangerooge, East Frisian Islands (between 3.3 to 4m) and Westerland, Sylt Island (3.5 to 4m) in Germany, and at Blåvandshuk (4.5 to 5m) and Årgab (about 6m) in Denmark (Newig and Kelletat, 2011). There were a large number of reports of this tsunami along the English Channel, some of them of about 2.5m height. Yet the tsunami reports in Belgium and in the south of the Netherlands mention only about 1.25m height (Newig, 2012).

Newig and Kelletat (2011) conclude that the source of this tsunami was not in the English Channel itself but south of its entrance. They infer that the large tsunami run-ups in Germany and Denmark for the 1858 tsunami were due to the interference between the western wave (coming from the English

Channel) and the northern wave (coming from Scotland). Still, they recognize that the reports of tsunami heights were larger for the North Sea than for the English Channel. Our results from Section 5.1 agreed with these reports showing high damping of the Channel wave, therefore the interference as cause of larger run-up in Denmark and Germany, is unlikely. Additionally, the tsunami was reported to arrive in Germany about one hour later than in Denmark; therefore the higher run-ups in these countries were due to a wave coming from the north.

Among our results of Section 4 in the GBM, the maximum tsunami heights for the (e) and (f) cases were located at the north coast of East Frisian Islands, at the west coast of Sylt Island, both in Germany and at Blåvandshuk in Denmark (Figure 9e and Figure 9f). Årgab lays outside of the GBM so we were not able to produce a good estimation of the maximum tsunami height there. Nevertheless, the refNSM results showed high tsunami heights offshore Årgab for cases (e) and (f), higher for the later than for the former (compare Figure 8e and Figure 8f). The differences in arrival times at those three locations for case (f) also matched better the 1858 reports than for case (e), Figure 11.
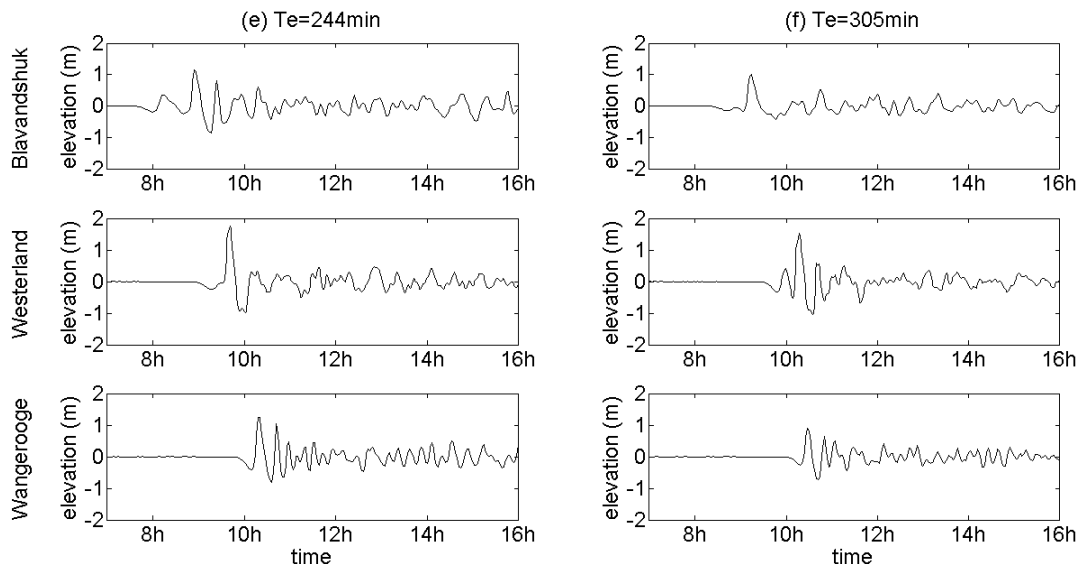

Figure 11. Time series of water height, in meters, on Blåvandshuk (Denmark), Westerland and Wangerooge (German Frisian Islands) for cases (e) and (f) of Section 5.2.

The leading depression of the tsunami wave at Blåvandshuk, Westerland and Wangerooge stations (Figure 11) was much smaller than the subsequent elevation; this could be the reason for no leading depression reported by eyewitnesses in those places (Newig and Kelletat, 2011). The reports of the 1858 tsunami run-up are higher for Blåvandshuk than for Westerland and Wangerooge, and our model system obtained higher runups for Westerland than for the other two places. The difference may be due to inaccuracies in the witnesses' reports, or the tide at the moment the tsunami arrived. We performed a simple analysis of the influence of tides on tsunami heights in Section 7 and found that they were affected by the tidal phase.

The timeline and wave height of the tsunami observations and our modeling results point that the wave that arrived in the south of the Netherlands was probably the damped western wave and it was too small to be noticed at German shores. Few hours later, the northern wave arrived to Denmark and then to Germany, with a direction of incidence similar to case (f), corresponding to an origin further east of the 1755 tsunami source given by NOAA (NGDC, 2012): 36°N and 11°W. Other authors propose epicentres further east for the 1755 earthquake, for example Moreira (1989), Reid (1914) and Zitellini (1999), all at 10°W. Also, the tsunami source could have been at Biscay Bay or offshore from Morocco.

Horsburgh et al. (2008) simulated several scenarios of tsunamis arriving at the United Kingdom shores from the offshore region of the Iberia Peninsula. They concluded that the Galician Rise shields Ireland and the west coast of Great Britain and also that the extent of the continental shelf dissipates energy of tsunamis coming from the south before they reach these coasts. However, they did not model the tsunamis at Scotland or their entrance to the North Sea. From the arrival time chart of the 1755 Lisbon tsunami (NGDC, 2012) we know that tsunamis coming from the south propagate north along the continental slope and through the Rockall Trough at high velocities, and then get refracted around Scotland and enter the North Sea. As the propagation along the continental slope and the Rockall Trough occur at great ocean depths, it is very likely that this wave experiences very little energy loss.

8. COMPARISON OF STORM SURGES AND TSUNAMIS

Storms are common phenomena in the North Sea. The surges they provoke have caused inundations and damages at the German coast, thus dikes have been built along the entire coastline to protect the coastal population. Tsunamis, on the other hand, are much less frequent and they are not taken into account in preventive measures and are not present in people's memory, either.

In Figure 12, we compare the water levels and depth-averaged flow velocities caused by storm surges and tsunamis at Westerland station, on Sylt Island, because this station presented the highest heights on all the tsunami simulations performed as described in previous sections. We plotted the storm surges of February 1967, January 1976 and December 1999, which were simulated as part of the validation in Section 3. For tsunamis, we plotted the Storegga like tsunami modeled in Section 4, and the case (f) of Section 5.2. Storm surges have much larger durations than the two tsunamis shown in the paper. Although landslide-generated tsunami had larger duration and period than earthquake-generated tsunami, their duration is still much shorter than that of storm surges.

The heights for the Storegga tsunami were about half than those for the storm surges. The tsunami wave of Section 5.2 was also smaller than the storm surges, yet it was generated employing a wave of unitary height at the refNSM boundary; therefore if the incoming wave is higher, this tsunami wave could be also higher. Additionally, the magnitude of the depth-averaged flow velocity for this tsunami was about double than for storm surges. The maximum magnitude of depth-averaged flow velocity for case (f) of Section 5.2 was of 1.6m/s, for the Storegga tsunami was of 0.48m/s and for the 1967, 1976 and 1999 storm surges was of 0.74, 0.68 and 0.61m/s respectively. Then, even when the tsunamis last

much less and their water levels are smaller, their flow velocities can be larger than the storm surges causing more damage.
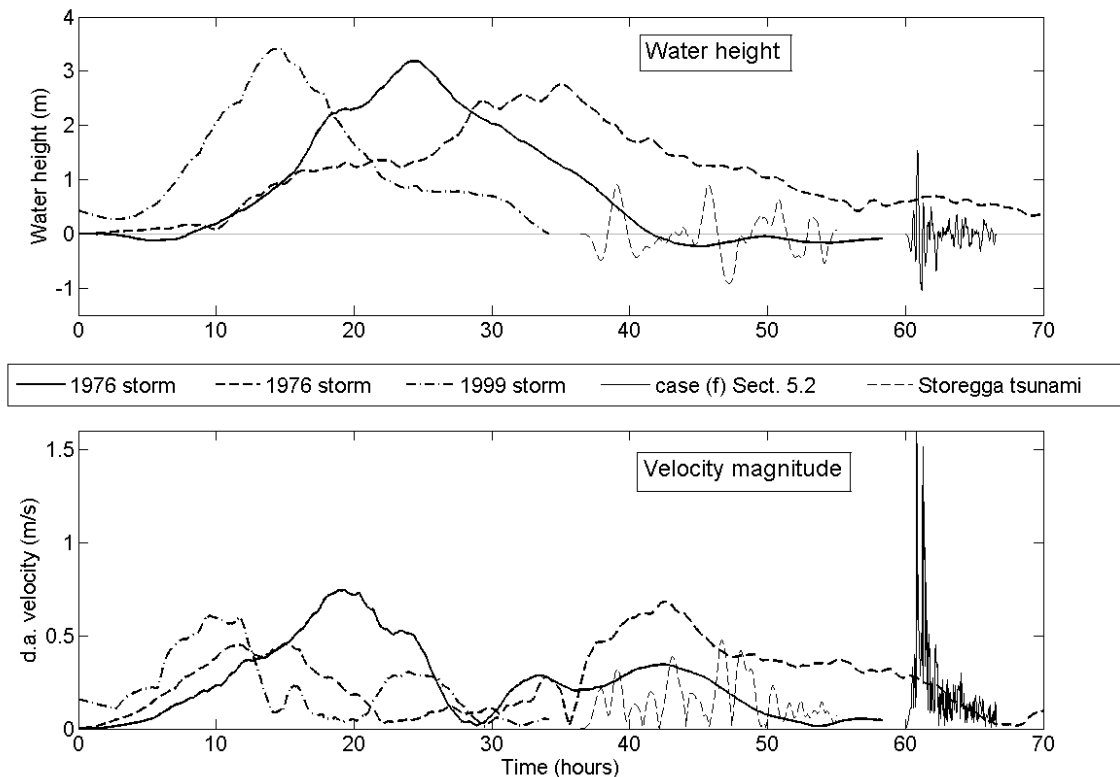

Figure 12. Comparison of storm surges and tsunamis on Westerland station, Sylt Island. The upper panel plots water levels and the bottom panel plots depth-averaged flow velocity magnitude. The times were shifted to show the differences more clearly.

9. TSUNAMIS AND TIDES

Tides have been proven to have an impact on storm surges in the North Sea (Bruss et al., 2010). Tsunamis are usually modeled without considering tidal influence; however, tides have been also proven to impact on tsunami heights (Kowalik et al., 2006) and (Kowalik and Proshutinsky, 2010). Kowalik and Proshutinsky (2010) superimposed tsunami signals on different stages of the tide on a simple slope channel to explore the influence of tides on tsunamis. The largest tsunami heights resulted during ebbing and low tide, because the change in bottom friction due to the interaction of tsunami and tides was larger at those stages. They conclude that under real conditions, the interaction of tsunami and tides is non-linear and it is given in terms of bottom friction, advection and momentum flux along with changing depths and velocities. Finally, they recommend tides to be simulated together with tsunamis in places where the former are comparable to prevailing depths, as it is the case for the North Sea. Therefore we superimposed an N-wave to the spring tide of August 14th 1999 to explore the influence of tides on tsunamis heights. To obtain the tidal forcing for the refNSM, we

imposed an astronomical forcing at the open boundaries of a larger model: the Continental Shelf Model (CSM) of Verboom et al. (1992). The resulting water levels and current velocities at the refNSM boundaries were used to obtain the Riemann-invariant boundary condition for 9 days of simulation. The N-wave of Section 5.2, case (a) of normal incidence, was superimposed to the tides on two different moments, such that the tsunami arrived at Cuxhaven station during high tide and low tide. This procedure was only performed for the north open boundary, on the west open boundary only the tide was prescribed. Then, the tide was subtracted from the model results of the sum of tides and tsunami, and this residual was compared with the tsunami results of Section 5.2 case (a) at Cuxhaven station. If the interaction between tsunamis and tides were linear, the residual should be equal to the tsunami modeled alone.

The results for the two cases, high tide and low tide, are compared in Figure 13: pure tsunami with thin lines and tsunami under the influence of tides with thick lines. The influence of tides and its phase on tsunami heights was remarkable. The differences between the pure tsunami and the tide-influenced tsunami were higher if the tsunami arrived during low tide than if it arrived during high tide, agreeing with the results from Kowalik and Proshutinsky (2010) for tsunamis and Bruss et al. (2010) for storm surges. However, despite the tidal phase, the pure tsunami signal presented higher heights than the tide-influenced tsunami. It is not possible to predict a tsunami event and therefore it is not possible to superimpose the right tide forcing when tsunamis are simulated. In this case, the modeling of the tsunami alone could be considered as a reasonable approximation to the maximum possible tsunami height at Cuxhaven. Still, to generalize this result more research would be desirable considering other tidal phases, tsunami frequencies and heights, and locations along the German Bight.
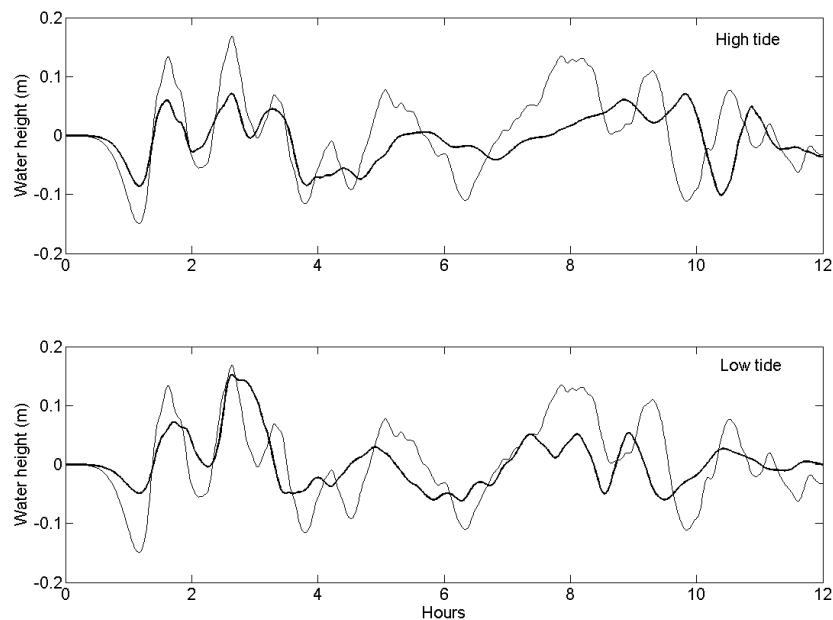
Figure 13. Influence of tides and tidal phase on tsunamis. Comparison of tsunami heights obtained without considering tides (thin line) and tsunami heights obtained taking tides into account (thick line).

10. CONCLUSIONS

Tsunami risk in the North Sea was explored by means of N-waves imposed at the open boundaries of the refined North Sea model. Each tsunami affected different regions on the North Sea basin and the German Bight. For the German Bight, among all cases analyzed, the most dangerous tsunamis were those generated by earthquakes south of the North Sea, because of their incidence direction. Particularly for the 1858 tsunami, the location of the most affected regions and their arrival times along the German Bight and Denmark were well reproduced. Our results indicated that the reason for the highest heights reported for this tsunami in this region was directionality rather than wave interference. This directionality points to a source for this tsunami further east from the Gorringer Banks.

The type of tsunami source was found to play an important role determining the most affected regions. Submarine slides generated tsunamis and earthquake generated tsunamis differ not only in their characteristic amplitudes but also in frequency and shape. Those differences were remarkable as the Storegga-like tsunami and an earthquake generated tsunami imposed in the same way affected different regions in the German Bight and the North Sea.

The interaction of tsunamis and tides was tested using one tsunami case in two tidal phases. The results showed that for the North Sea this interaction is clearly non-linear. The tsunami heights were higher for the tsunami arriving during low tide; however the tsunami heights without considering tides were the highest ones. More experiments considering other tidal phases, tsunami characteristics and stations would be necessary to generalize this result.

The highest tsunami heights reported in history at the German Bight are about 4m, comparable to the maximum storm surge recorded at this region. However, it was found that the depth-averaged flow velocity generated by tsunamis was comparable or larger than that generated by storm surges, suggesting that a large tsunami may cause more damage than a storm surge. Therefore, tsunamis should not be dismissed as a threat for the German Bight.

REFERENCES

Apotsos, A., Buckley, M., Gelfenbaum, J., Jaffe, B. and Vatvani, D. (2011a), Nearshore tsunami inundation model validation: towards sediment transport applications, Pure and Applied Geophysics, doi:10.1007/ss00024-011-0291-5.

Apotsos, A., Gelfenbaum, G. and Jaffe, B. (2011b), Process-based modeling of tsunami inundation and sediment transport, Journal of Geophysical Research - Earth Surface, 116, (F01006), doi:10.1029/2010JF001797.

Apotsos, A., Jaffe, B. and Gelfenbaum, G. (2011c), Wave characteristic and morphologic effects on the onshore hydrodynamic response of tsunamis, Coastal Engineering, 58, 1034-1048, doi:10.1016/j.coastaleng.2011.06.002.

Apotsos, A., Jaffe, B., Gelfenbaum, G. and Elias, E. 2009, 'Modeling time-varying tsunami sediment deposition', Proceedings of Coastal Dynamics 2009, Tokyo, doi:10.1145/9789814282475_0037.

Borck, I., Dick, S., Kleine, E. and Müller-Navarra, E. 2007, 'Tsunami - a study regarding North Sea coast', Nr. 41/2007, Bundesamt für Seeschiffahrt und Hydrographie, Hamburg and Rostock.

Bruss, G., Gönnert, G. and Mayerle, R. 2010, 'Extreme scenarios at the German North Sea Coast. A numerical model study.', Coastal Engineering, Shangai, China.

Carrier, G.F, Wu, T.T and Yeh, H. (2003), Tsunami run-up and draw-down on a plane beach, Journal of Fluid Mechanics, 475, 79-99.

Dawson, A.G. (1999), Linking tsunami deposits, submarine slides and offshore earthquakes, Quaternary International, 60, 119-126.

Gelfenbaum, G., Vatvani, D., Jaffe, B. and Dekker, F. 2007, 'Tsunami inundation and sediment transport in vicinity of coastal mangrove forest', Coastal Sediments 2007, American Society of Civil Engineers (ASCE), New Orleans.

Harbitz, C.B (1992), Model simulations of tsunamis generated by the Storegga Slides, Marine Geology, 105, 1-21.

Hartsuiker, G. 1997, 'Deutsche Bucht and Dirthmarscher Bucht, Set-up and Calibration of Tidal Flow Models', Delft Hydraulics, Report H1821, Delft.

Horsburgh, K.J, Wilson, C., Baptie, B.J, Cooper, A., Cresswell, D., Musson, R.M.W, Ottemöller, L., Richardson, S. and Sargeant, S.L (2008), Impact of a Lisbon-type tsunami on the U.K. coastline and the implications for tsunami propagation over broad continental shelves, Journal of Geophysical Research, 113, C04007, doi:10.1029/2007JC004425.

Imamura, F. and Goto, C. (1988), Truncation error in numerical tsunami simulation by the finite differences method, Coastal Engineering in Japan, 31, 245-263.

Kowalik, Z. and Proshutinsky, A. (2010), Tsunami-tide interactions: a Cook Inlet case study, Continental shelf research, 30, 633-642, doi:10.1016/j.csr.2009.10.004.

Kowalik, Z., Proshutinsky, T. and Proshutinsky, A. (2006), Tide-tsunami interactions, Science of Tsunami Hazards, 24:4, 242-256.

Leeser, G.R., Roelvink, J.A, van Kester, J.A.TM and Stelling, G.S (2004), Development and validation of a three-dimensional morphological model, Coastal Engineering, 51, 883-915.

Lehfeldt, R., Milbradt, P., Plüss, A. and Schüttrumpf, H. (2007), Propagation of a Tsunami-Wave in the North Sea, Die Küste, 72, 105-123.

Mayerle, R., Wilkens, J., Escober, C. and Windupranata, W. (2005), Hydrodynamic Forcing Along the Open Sea Boundaries of Small-Scale Coastal Models, Die Küste. Archive for research and technology on the North Sea and Baltic Coast, 69, 203-228.

Moreira, V.S 1989, 'Seismicity of the Portuguese continental margin', in S Gregersen, PW Basham (eds.), Earthquakes at North Atlantic Passive Margins Neotectonic and Postglacial Rebound, Kluwer, Massachusetts.

NEWIG, J. 2012. Personal Communication.

Newig, J. and Kelletat, D. (2011), The North Sea tsunami of June 5, 1858, Journal of Coastal Research, 27:5, 931-941, doi:10.2112/JCOASTRES-D-10-00098.1.

NGDC. 2012. Tsunami Travel Time Maps. [online]. [Accessed 2012]. <http://www.ngdc.noaa.gov/hazard/tsu_travel_time.shtml>

NGDC/WDC 2012, Global Historical Tsunami Database, viewed 2012, <http://www.ngdc.noaa.gov/hazard/tsu_db.shtml>.

Pritchard, D. and Dickinson, L. (2008), Modelling the sedimentary signature of long waves on coasts: implications for tsunami reconstruction, Sedimentary Geology, 206, 42-57, doi:10.1016/j.sedgeo.2008.03.004.

Reid, H.F (1914), The Lisbon earthquake of November 1 1755, Bull. Seismological Society of America, 4, 53-80.

Smith, D.E, Shi, S., Cullingford, R.A, Dawson, A.G, Dawson, S., Firth, C.R, Foster, I.DL, Fretwall, P.T, Haggart, B.A, Holloway, L.K and Long, D. (2004), The Holocene Storegga Slide tsunami in the United Kingdom, Quaternary Science Reviews, 23, 2291-2321, doi:10.1016/j.quascirev.2004.04.001.

Synolakis, C.E, Bernard, E.N, Titov, V.V, Kanoglu, U. and Gonzalez, F.I (2008), Validation and Verification of Tsunami Numerical Models, Pure and Applied Geophysics, 165, 2197-2228.

Tadepalli, S. and Synolakis, C.E. (1996), Model for the leading waves of tsunamis, Physical Review Letters, 77:10, 2141-2144.

Vatvani, D., Boon, J. and Ramanamurty, P. 2005, 'Flood risk due to tsunami and tropical cyclones and the effect of tsunami excitations on tsunami propagations', Proc. of the IAEA Workshop on External Flooding Hazards at NNPS, Kalpakkam - Tamil Nadu.

Verboom, G., Ronde, J. and Dijk, R. (1992), A fine grid tidal flow and storm surge model of the North Sea., Continental Shelf Research, 12:2, 213-233.

Verboom, G.K and Slob, A. (1984), Weakly-reactive boundary conditions for two-dimensional water flow problems, Advances in water resources, 7:4, 192-197.

Zitellini, N., Chierici, F., Sartori, R. and Torelli, L. (1999), The tectonic source of the 1755 earthquake and tsunami, Ann. Geofis., 42, 49-55